İSTANBUL ÜNİVERSİTESİ YAYINEVİ

**RESEARCH / ARAŞTIRMA**
DOI: 10.26650/IUITFD.2019.0082
İst Tıp Fak Derg 2020 / J Ist Faculty Med 2020

# VARIABLE ANATOMY OF THE INFRATROCHLEAR AND SUPRATROCHLEAR TRIANGLES AND THEIR MICRONEUROSURGICAL IMPORTANCE

## İNFRATROKLEAR VE SUPRATROKLEAR ÜÇGENLERİN VARYATİF ANATOMİSİ VE MİKRONÖROCERRAHİ ÖNEMİ

İlke Ali GÜRSES[1], Osman COŞKUN[1], Özcan GAYRETLİ[1], Ayşin KALE[1], Adnan ÖZTÜRK[1]

[1]Istanbul University, Istanbul Faculty of Medicine, Department of Anatomy, Istanbul, Turkey

**ORCID IDs of the authors:** İ.A.G. 0000-0001-9188-4662; O.C. 0000-0002-0337-4927; Ö.G. 0000-0001-7958-3170; A.K. 0000-0002-2305-420X; A.Ö. 0000-0002-5819-0543

**Cite this article as:** Gurses IA, Coskun O, Gayretli O, Kale A, Ozturk A. Variable anatomy of the infratrochlear and supratrochlear triangles and their microneurosurgical importance. J Ist Faculty Med 2020;83(4):355-62. doi: 10.26650/IUITFD.2019.0082

## ABSTRACT

**Objective:** Supratrochlear and infratrochlear triangles are surgical corridors for approaching the lateral wall of the cavernous sinus. The literature provides conflicting results for the morphology and morphometry of these triangles. Additionally, the possible effects of vascular structures that drain into the cavernous sinus in unknown. This study aimed to investigate the morphology, morphometry, and vascular relationships of the supratrochlear and infratrochlear triangles of the cavernous sinus.

**Material and Method:** Cranial bases of 25 cadavers were dissected bilaterally under a surgical microscope. Five of the cadavers were injected with colored silicone for vascular evaluation. The morphology of supratrochlear and infratrochlear triangles were classified according to the course of the trochlear nerve. Photogrametric measurements were used for evaluating the areas of both triangles with the ImageJ software. The triangular morphology was also investigated in regard to the drainage patterns of the superficial middle cerebral vein and cranial base dural sinuses.

**Results:** Type A, B, C, and D triangle morphology was present on 23 (46%), 9 (18%), 10 (20%), and 8 (16%) sides, respectively. The average areas for supratrochlear and infratrochlear triangles were 22.2 (±11.7) $mm^2$ and 78.4 (±27.7) $mm^2$, respectively. The supratrochlear triangle was significantly larger in Type D triangles. On 71.4% of injected specimens, the superior petrosal sinus contributed the cavernous sinus and formed a Type A triangle.

**Conclusion:** The anatomy of the supratrochlear and infratrochlear triangles are highly variable than previously reported. Introducing the knowledge regarding these variations to neurosurgical residency education programs and daily surgical practice could be valuable.

**Keywords:** Cavernous sinus, supratrochlear triangle, infratrochlear triangle

## ÖZET

**Amaç:** Supratroklear ve infratroklear üçgenler, sinus cavernosus'un lateral duvarına ulaşmak için kullanılabilecek cerrahi koridorlardır. Literatürde bu üçgenlerin morfolojisi ve morfometrisi hakkında çelişkili bilgiler bulunmaktadır. Ayrıca, sinus cavernosus'a drene olan vasküler yapıların anatomiye olan etkileri bilinmemektedir. Bu çalışma sinus cavernosus üçgenlerinde olan supratroklear ve infratroklear üçgenlerin morfolojisini, morfometrisini ve vasküler komşuluklarını incelemeyi amaçlamıştır.

**Gereç ve Yöntem:** Yirmibeş kadavranın kafa tabanı cerrahi mikroskop altında bilateral olarak disseke edildi. Vasküler yapıların değerlendirilmesi amacıyla 5 kadavrada renkli silikon enjeksiyonu yapıldı. Supratroklear ve infratroklear üçgen morfolojisi, n. trochlearis'in uzanımına göre sınıflandırıldı. Her iki üçgenin alanları, ImageJ yazılımı kullanılarak fotogrametrik yöntem ile ölçüldü. Üçgenlerin morfolojisi ile v. cerebri media superficialis ve kafa tabanı dural sinüslerinin drenaj paterni karşılaştırıldı.

**Bulgular:** Tip A, B, C ve D üçgen morfolojisi sırasıyla 23 (%46), 9 (%18), 10 (%20) ve 8 (%16) tarafta gözlemlendi. Supratroklear ve infratroklear üçgenlerin ortalama alanları 22,2 (±11,7) $mm^2$ ve 78,4 (±27,7) $mm^2$ ölçüldü. Tip D üçgenlerde supratroklear üçgenin daha büyük olduğu görüldü. İnjeksiyon yapılan örneklerin %71,4'ünde sinus petrosus superior, sinus cavernosus'a drene olmakta ve belirgin Tip A üçgen meydana getirmekteydi.

**Sonuç:** Supratroklear ve infratroklear üçgenler, literatürde raporlandığının aksine çok varyatifti. Bu çeşitlilik bilgisinin beyin cerrahisi uzmanlık eğitimi ve günlük cerrahi uygulamaya aktarılması düşünülebilir.

**Anahtar Kelimeler:** Sinus cavernosus, supratroklear üçgen, infratroklear üçgen

**Corresponding author/İletişim kurulacak yazar:** iagurses@gmail.com

**Submitted/Başvuru:** 27.09.2019 • **Revision Requested/Revizyon Talebi:** 24.03.2020 •
**Last Revision Received/Son Revizyon:** 16.04.2020 • **Accepted/Kabul:** 20.06.2020 • **Published Online/Online Yayın:** 05.10.2020

## INTRODUCTION

The oculomotor (CN-III), trochlear (CN-IV), and ophthalmic (CN-V1) nerves confine two triangular surgical corridors at the lateral wall of the cavernous sinus (CS) (1). The supratrochlear (STT) and infratrochlear triangles (ITT), which are named after their relative location to the CN-IV, are commonly used in lateral approaches to the CS (1-6).

Although the anatomy and morphometry of the ITT, also known as the Parkinson's triangle, had attracted many researchers (2, 7-13), morphologic studies that investigated both triangles are limited (9-11). The CN-IV constitutes borders for both triangles, therefore it is the major anatomical structure that affects the morphology. Lang and Reiter (10) classified the morphological patterns of these triangles according to the course of the CN-IV and found considerable variability (Figure 1). Studies that investigated the morphology of both triangles on different populations provide variable frequencies for morphological types, which could be attributed to ethnicity (9-11). Additionally, some studies that evaluated the morphometry of both triangles provide very similar averages for STT and ITT areas with little variability (2, 13). Apparently, there is a paucity of information on the morphology and morphometry of both triangles.

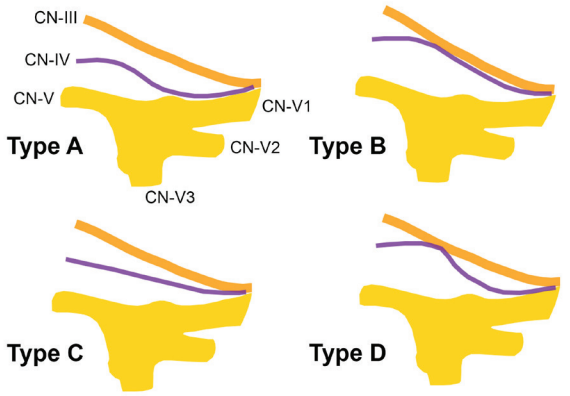


**Figure 1:** Schematic illustration depicting morphological types of supratrochlear and infratrochlear triangles. CN-III: Oculomotor nerve, CN-IV: Trochlear nerve, CN-V: Trigeminal nerve, CN-V1: Ophthalmic nerve, CN-V2: Maxillary nerve, CN-V3: Mandibular nerve. The figure is based on the classification of Lang and Reiter (10).

Additionally, it is well known that the CS is also a drainage point for the superficial middle cerebral vein (SMCV) (14, 15). Despite the anatomic detail provided on the STT and ITT in previous studies (2, 7-13), triangle anatomy in different venous patterns was not studied.

Therefore, this study was aimed to investigate the morphology and morphometry of the STT and ITT and to outline the relationships between these triangles and adjacent venous structures.

## MATERIAL AND METHOD

### Specimens and vascular injections

After ethical committee approval (date: 10.01.2018, number: 11), the morphology and morphometry of the STT and ITT were evaluated on 8 female and 17 male (total 25) cadavers. Sixteen cadavers were donors and 9 were of unclaimed origin. All specimens were obtained from the Department of Anatomy of Istanbul Faculty of Medicine either through the Body Donation Program of the department or legally procured under Act 2238 (16). All cadavers were preserved with a formalin-ethanol-glycerine-phenol solution and kept in cold storage (5-8 °C) after embalming. Average age at death was 60.9 (ranged between 26 and 85 years).

Among the sample, 5 cadavers were injected with colored silicone into the arteries (red) and veins (blue) according to the protocol reported by Sanan et al. (17) for evaluating the vascular anatomy of the CS.

### Dissection protocol and morphological evaluation

All dissections were performed under 6x to 25x magnification of a surgical microscope (D.F. Vasconcellos S.A., M 1222, Sao Paolo, Brazil). After removing the calvaria with an oscillating saw, the cerebrum was removed with great care and the dura covering the CS was kept intact. Cranial nerves from two through to six were cut at subarachnoid level and their dural entry points were preserved. For vascular evaluation, the bridging veins connecting the SMCV to the CS were cut after identification of that given vein. In most of the cases, the anterior clinoid process was drilled in order to evaluate anterior sections of both triangles. Finally, outer dura covering the CS was dissected with care. Dissection of the inner dural layer was only preferred if exposure of cranial nerves were not adequate. Dural entry points of CN-III, CN-IV, and CN-V1 to the lateral wall of the CS were preserved for morphometric evaluation.

The morphology of the STT and ITT was classified according to Lang and Reiter (10). In Type A, the CN-IV had a curved course at the CS and formed two ill defined triangles. In Type B, the CN-IV approximates superiorly to the CN-III and the STT was smaller than the ITT. In Type C, the CN-IV had a linear course at the CS and formed two well defined triangles. In Type D, the CN-IV was close to the CN-III proximally and to the CN-V1 distally. In this type, the STT had a bow shape, rather than a triangle (Figure 1).

Drainage pattern of the SMCV was evaluated according to the classification of Suzuki and Matsumoto (15) as sphenoparietal, cavernous, emissary, superior petrosal, basal, squamosal, and combined (Figure 2).

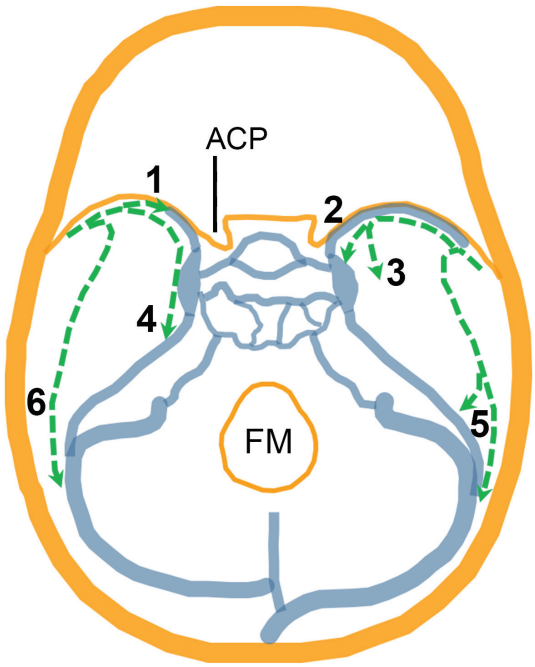


**Figure 2:** Schematic illustration of the cranial base summarizing the drainage patterns of the SMCV. Dotted green lines outline variated course of the SMCV. ACP: Anterior clinoid process, FM: Foramen magnum. The SMCV courses medial to the oval foramen and can drain into the sphenoparietal (1), cavernous (2), and the superior petrosal (4) sinuses directly. In emissary pattern (3), the SMCV drains into the emissary veins around the oval foramen. The SMCV can pass lateral to the oval foramen at the base of the middle cerebral fossa and drain into either the superior petrosal or the transverse sinuses in basal pattern (5). In squamous (6) pattern, the SMCV passes more laterally at the squama temporalis and drains into the transverse sinus. The illustration is based on the classification of Suzuki and Matsumoto (15).

### Measurements and statistical analysis

Morphometry of the triangles were evaluated with photogrametry. Digital photographs of the CSs were obtained from a distance of 20 cm for each specimen. A tape measure of 10 mm was placed in every CS for calibration of the image with an editing software. ImageJ (v1.46r, 2013, NIH, USA) (18) software was used to measure the areas of both triangles (Figure 3).

The data obtained from ImageJ was transferred to an excel file and statistical analysis was performed with SPSS v. 21.0 (IBM SPSS Statistics for Windows, NY; IBM Corp., 2012). Morphometrical differences between sexes, sides, and morphological triangle types were evaluated with Mann-Whitney U test. Values with $p<0.05$ was considered as statistically significant.

## RESULTS

### Morphology and morphometry

Type A, B, C, and D triangles were observed on 23 (46%), 9 (18%), 10 (20%), and 8 (16%) sides, respectively (Figure 4) (Table 1).

The average areas for STT and ITT were 22.2 (±11.7) $mm^2$ and 78.4 (±27.7) $mm^2$, respectively. The differences for both triangles among sexes and sides were not statistically significant (Table 2). For STT, Type D triangles had a statistically larger area compared to Types A ($p=0.03$), B ($p=0.002$), and C ($p=0.01$) triangles, respectively. For ITT, differences between areas among morphological types did not reach statistical significance (Table 3).

### Vascular relationships

Of 5 cadavers injected with colored silicone, optimal evaluation was possible on 9 sides. The SMCV drainage to the CS was cavernous type on 6 (66.7%), superior petrosal type on 1 (11.1%), emissary type on 1 (11.1%), and combined type on 1 (11.1%) side (Figure 5). The cavernous types drained into the CS through the anteromedial

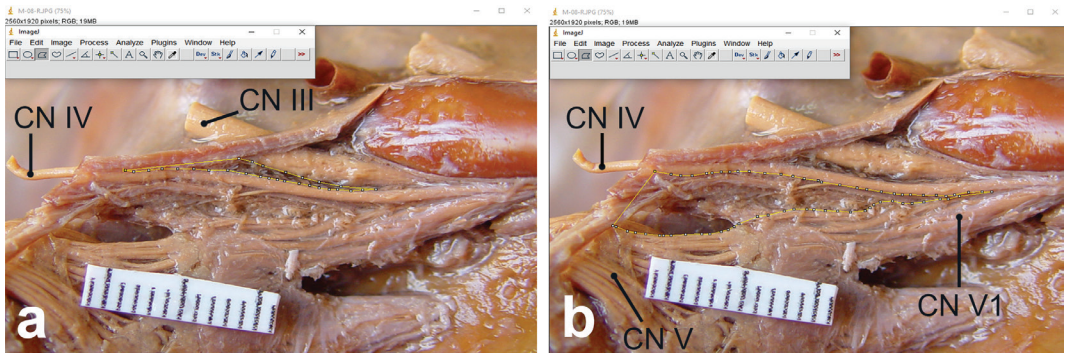


**Figure 3:** Figure shows area measurements for the supratrochlear (a) and infratrochlaer (b) triangles with the ImageJ software using the poligon selection tool. CN-III: Oculomotor nerve, CN-IV: Trochlear nerve, CN-V: Trigeminal nerve, CN-V1: Ophthalmic nerve.

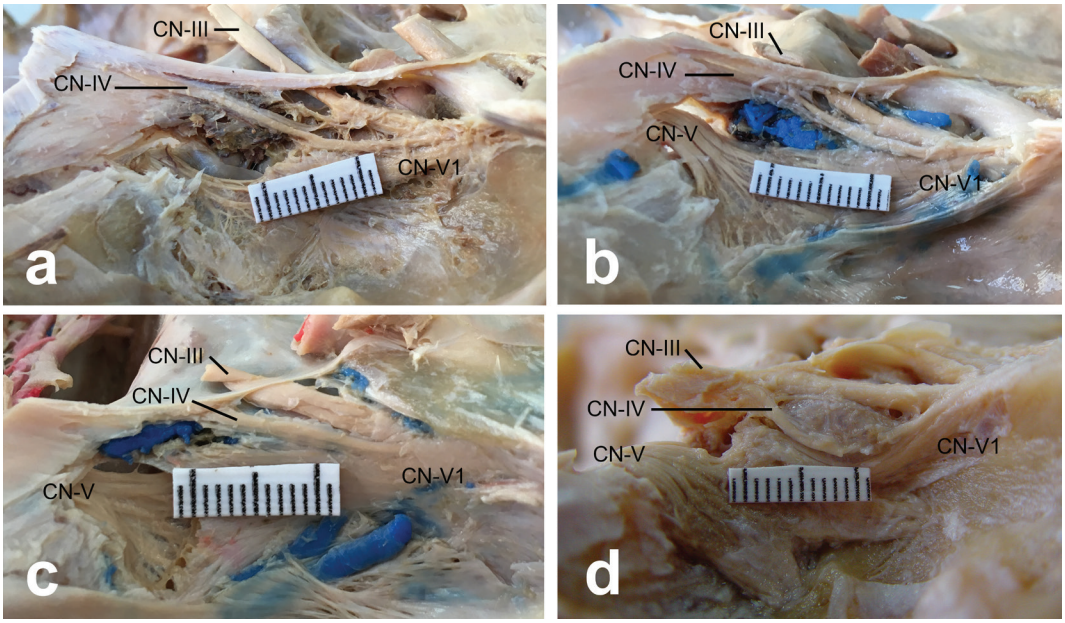


**Figure 4:** Type A (a), B (b), C (c), and D (d) triangle morphologies. CN-III: Oculomotor nerve, CN-IV: Trochlear nerve, CN-V: Trigeminal nerve, CN-V1: Ophthalmic nerve.

**Table 1:** Comparison of previous studies that evaluated supratrochlear and infratrochlear triangle morphology.

| Previous study, year | Number of cadavers / sides used | Morphological triangle type | | | | |
|---|---|---|---|---|---|---|
| | | Type A | Type B | Type C | Type D | Type E |
| Lang and Reiter, 1984 (10) | 86 sides | 53.5% | 31.4% | 8.1% | 7% | - |
| Miyazaki et al., 1994 (11) | 50 sides (10 adults, 20 tissue blocks) | 15% | 60% | 15% | 5% | 5% |
| Kayalioglu et al., 1999 (9) | 108 sides (54 cadavers) | 35.2% | 30.8% | 18.5% | 6.5% | - |
| Present study, 2019 | 50 sides (25 cadavers) | 46% | 18% | 20% | 16% | - |

**Table 2:** Comparison of supratrochlear and infratrochlear triangle areas regarding sex and side.

| | Sex | | Significance (p) |
|---|---|---|---|
| | Female | Male | |
| **Supratrochlear** | 24.2±12.9 | 21.5±15.4 | >0.05 |
| **Infratrochlear** | 79.1±29.7 | 78.1±27.3 | >0.05 |
| | **Side** | | |
| | **Right** | **Left** | |
| **Supratrochlear** | 25.5±16.4 | 19±12.3 | >0.05 |
| **Infratrochlear** | 76.8±28 | 79.9±27.9 | >0.05 |

triangle (Figure 5). The combined type had two SMCVs, one with cavernous and the other with superior petrosal drainage. Additionally, on 7 sides the superior petrosal sinus had contributed to the CS. On 5 out of 7 cases (71.4%) the CN-IV was relocated superiorly and formed a Type A triangle (Figure 5). Nevertheless, the sample size of vascular specimens was not large enough for statistical evaluation.

**Table 3:** Comparison of supratrochlear and infratrochlear triangle areas regarding morphological types.

| | Supratrochlear[a] | Infratrochlear[b] |
|---|---|---|
| **Type A** | 22.7±14.7 | 77±26.1 |
| **Type B** | 14.1±6.4 | 83.4±28.2 |
| **Type C** | 17.1±8.7 | 83.4±37 |
| **Type D** | 36.3±18.3 | 70.3±20.1 |

[a]Areas of Type D triangles were significantly larger than Type A (p=0.03), B (p=0.002), and C (p=0.01) triangles.
[b]Area differences between morphological types did not reach significance level.

IV and the CN-V1 enables the surgeon to enlarge both triangles and expose the abducens nerve and the lateral venous space (5, 19). Moreover, Knosp et al. (23) argued that approaching CS meningiomas through the ITT provided more space to work for the neurosurgeon. Therefore, the course of the CN-IV gains importance for the microneurosurgical approaches to the cavernous sinus.

There are a few preferred surgical approaches for resecting tumors in and around the CS (20). A cranio-orbito-zygomatic approach allows wide exposure of the entire CS with minimal brain retraction (20, 21), while an extended middle fossa approach is used in cases with a tumor at

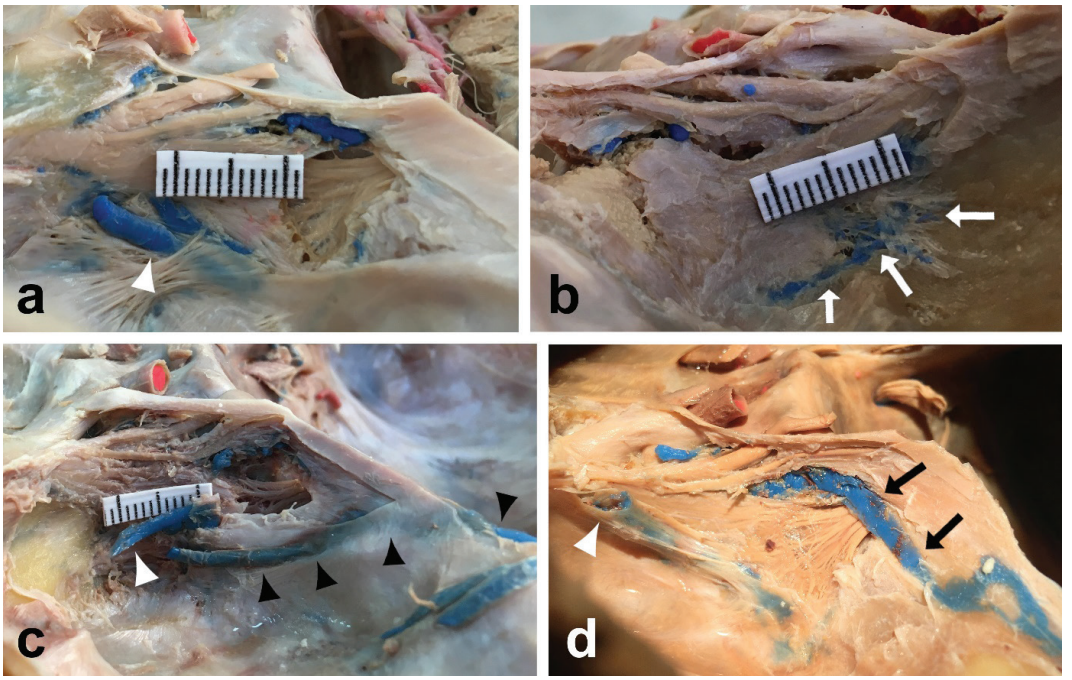


**Figure 5:** Cavernous (a), emissary (b) and combined (c) venous drainage patterns observed in the study. When the superior petrosal sinus contributed to the CS (black arrows), CN-IV was pushed superiorly and formed a Type A triangle morphology (d). White arrowheads depict cavernous, black arrowheads depict superior petrosal, and white arrows depict emissary drainage patterns.

## DISCUSSION

The ITT, which was described by Parkinson (3, 4) as a direct entry route to the CS, forms a common surgical corridor at the lateral wall of the CS (5, 19). Through this triangle, it is possible to expose the posterior vertical segment, posterior bend, and the horizontal segment of the internal carotid artery, the meningohypophyseal trunk, posterosuperior and lateral venous spaces, and the lateral wall of the pituitary gland (2, 5, 19-22). Conversely, the STT is a narrow triangle that could be used for accessing the branches of the meningohypophyseal trunk (5). Despite the STT being narrow, dissection and retraction the CN-

the posterior CS (21, 24). An additional lateral sphenoidectomy, extended middle fossa approach also provides tumor resection in cases with petrous apex or Meckel's cave involvement (24). A lateral intradural approach allows wide exposure of the CS, especially where the CS is occupied and/or compressed by tumor resulting in lateral wall distortion or enlargement (20). However, this approach prevents direct visualization of the entry points of the cranial nerves at the lateral CS wall, thus increasing postoperative complications (5, 6, 19, 20). Conversely, an extradural approach provides a complete exposure of the tumor bed (20-22). Additionally, working between the

outer and inner dural layers of the lateral wall enables tumor resection without compromising the blood supply of adjacent cranial nerves (20, 21). In selected patients, a medial (transsellar) or lateral (transpterygoid) extradural endoscopic endonasal approach has been reported to yield higher clinical symptom recovery and cranial neuropathy improvement rate especially in cases with invasive adenomas of the CS (25-28).

Although classical texts (5, 19) mention the STT being the smaller triangle, previous literature reports either similar (13) or larger (2) areas for the STT (Table 4). Isolan et al. (2) also reported minimal variability for STT and ITT areas. The results of this study contradicts previous studies and found that the STT was larger and areas for both triangles were highly variable (Table 4). Given the complex and variable course of the CN-IV (10), it is possible for previous studies, which only provided linear measurements for nerves that do not traverse the lateral wall of the CS linearly, to miscalculate triangle areas. The variable anatomy of both triangles described by Lang and Reiter (10), urged the researchers to use a more reliable method of measurement (i.e. photogrametry) (18). Therefore, this study proposes that the areas for both triangles may be larger than previously reported. Moreover, this study showed that, especially in Type D morphology, the STT was siginificantly larger. During surgery, a relatively smaller ITT might require additional CN-IV dissection and retraction. Transient and permanent nerve damage due to CS surgery is uncommon (30). The major factors responsible for nerve damage are anatomical distortion of the region or direct involvement of neurovascular structures due to underlying pathologies such as meningiomas and aneurysms (20, 23, 30). Nevertheless, extensive manupilation of cranial nerves for imperative exposure during CS surgery might cause new nerve damages (30). In order to prevent this, combining different approaches such as extradural-lateral or extradural-superior approaches could be utilized for distorted cranial nerves with preoperative planning (20).

The CS is the primary venous drainage crossroad for the perisylvian cerebral regions, orbit, and the skull base (14). The SMCV constitutes the major venous structure that drains at the lateral wall of the CS (15, 31). It can drain into the anterior venous space via the sphenopareital sinus, the lateral venous space directly, or the posterosuperior venous space via the superior petrosal sinus (14, 15, 31). In this study, the superior petrosal type SMCV drainage was observed only in one case. Nevertheless, in the majority of cases (71.4%) where the superior petrosal sinus contributed to the cavernous sinuses, Type A morphology was observed. This might indicate that the venous drainage pattern of superficial veins into the CS might affect the CN-IV anatomy. However, this study could not support this finding with statistical significance. Thus, studies with larger sample sizes investigating whether the venous anatomy involves in triangle morphology are needed in the future.

Apart from therapeutic applications, understanding the complex anatomy of the CS has educational challeng-

**Table 4:** Comparison of anatomic studies that investigated the morphometry of infratrochlear and supratrochlear triangles.

| Previous study, year | Medial border[a] | Lateral border[a] | Base[a] | Area[b] |
|---|---|---|---|---|
| **Supratrochlear triangle** | | | | |
| Watanabe et al., 2003 (13) | 10.9±4.1 | 14±3.8 | 7±2.1 | 34.1±15.1 |
| Isolan et al., 2007 (2) | 13.18±3.19 | 14.27±1.35 | 5.51±0.82 | 36.46±4.34 |
| Present study, 2019 | - | - | - | 22.2±11.7 |
| **Infratrochlear triangle** | | | | |
| Harris & Rhoton, 1976 (7) | 13 | 14 | 6 | - |
| Sekhar et al., 1987 (12) | 17 | 17 | 5 | - |
| Inoue et al., 1990 (8) | 16.4 | 16.5 | 4.5 | - |
| Miyazaki et al., 1994 (11) | 12 | 13 | 4 | - |
| Day & Tschabitscher, 1996 (29) | 10.48 | 11.79 | 6.94 | - |
| Watanabe et al., 2003 (13) | 13.1±2.8 | 16.4±3.2 | 6.2±1.4 | 35.6±14.6 |
| Isolan et al., 2007 (2) | 10.29±0.99 | 12.33±1.19 | 4.34±0.44 | 21.06±4.56 |
| Present study, 2019 | - | - | - | 78.4±27.7 |

[a]Values for the borders of both triangles are presented as Mean±SD in mm.
[b]Values for triangle areas are presented as Mean±SD in $mm^2$.

es, such as low accessibility of cadaveric specimens for training, available educational material with poor detail or orientation, and decreased observation opportunities during noninvasive approaches (16, 20). Therefore, new educational models that has more accurate anatomical knowledge, are easily accessible, and are reusable were needed. Chung et al. (32) had provided a detailed schematic and a three dimensional model of the surgical triangles around the CS based on the segmentation of sectional cadaveric data (33, 34) and previous cadaveric studies (1, 2, 13, 35). This model allowed neurosurgery residents to simulate and study interhemispheric, pterional, middle cranial fossa, and retrosigmoid suboccipital approaches (32). Similarly, Qian et al. (36) have produced a three dimensional virtual reality model of the sellar region from cadaveric computed tomography data for neurosurgical residency training. Both educational models provide a convenient opportunity to observe complex spatial relationships and to perform basic skills. Nevertheless, adding further detail, including the variable anatomy of both triangles and venous structures into educational models may present an opportunity for advancing the neurosurgical training by increasing the anatomical accuracy and individuality.

A limitation of this study was its relative small sample size that was used to evaluate vascular anatomy. Some of reported venous drainage patterns were not observed. Additionally, a statistical comparison was not possible between venous drainage types and triangle morphologies. Therefore, the results should be taken as descriptive rather than definitive.

## CONCLUSION

The morphology and morphometry of supratrochlear and infratrochlear triangles show siginificant variability. The supra-trochlear triangle is larger in cases with Type D triangle morphology. Although Type A triangle morphology was frequent in cases with superior petrosal contribution to the CS, future studies that compares different venous drainage patterns and triangle morphologies are needed.

**Acknowledgements:** The authors are deeply grateful to the (unclaimed and donated) cadavers for providing this research opportunity.

**Ethics Committee Approval:** This study was approved by the Ethical Committee of the Istanbul University Istanbul Faculty of Medicine (Date: 10.01.2018, Number: 11).

**Informed Consent:** Written consent was not obtained from the participants. (Cadaver study)

**Peer Review:** Externally peer-reviewed.

**Author Contributions:** Conception/Design of Study- İ.A.G., O.C.; Data Acquisition- İ.A.G., Ö.G.; Data Analysis/Interpretation- A.K., A.Ö.; Drafting Manuscript- İ.A.G., O.C.; Critical Revision of Manuscript- Ö.G., A.K., A.Ö.; Final Approval and Accountability- İ.A.G., O.C., Ö.G., A.K., A.Ö.

**Conflict of Interest:** Authors declared no conflict of interest.

**Financial Disclosure:** This work was supported by the grant of Scientific Research Projects Coordination Unit of Istanbul University (Project No: TSA-2016-20144).

**Teşekkür:** Yazarlar olarak, bu araştırma imkanını sağlayan kimsesiz ve bağış kadavralara gönülden minnettarız.

**Etik Komite Onayı:** Bu çalışma için etik komite onayı İstanbul Üniversitesi İstanbul Tıp Fakültesi Etik Kurulu'ndan alınmıştır (Tarih: 10.01.2018, Numara: 11).

**Bilgilendirilmiş Onam:** Katılımcılardan bilgilendirilmiş onam alınmamıştır. (Kadavra çalışması)

**Hakem Değerlendirmesi:** Dış bağımsız.

**Yazar Katkıları:** Çalışma Konsepti/Tasarım- İ.A.G., O.C.; Veri Toplama- İ.A.G., Ö.G.; Veri Analizi/Yorumlama- A.K., A.Ö.; Yazı Taslağı- İ.A.G., O.C.; İçeriğin Eleştirel İncelemesi-Ö.G., A.K., A.Ö.; Son Onay ve Sorumluluk- İ.A.G., O.C., Ö.G., A.K., A.Ö.

**Çıkar Çatışması:** Yazarlar çıkar çatışması beyan etmemişlerdir.

**Finansal Destek:** Bu çalışma İstanbul Üniversitesi Bilimsel Araştırma Projeleri Koordinasyon Birimi hibesi ile desteklenmiştir (Proje Numarası: TSA-2016-20144).

## REFERENCES

1. Dolenc V. Direct microsurgical repair of intracavernous vascular lesions. J Neurosurg 1983;58(6):824-31. [CrossRef]
2. Isolan GR, Krayenbühl N, de Oliviera E, Al-Mefty O. Microsurgical anatomy of the cavernous sinus: measurements of the triangles in and around it. Skull Base 2007;17(6):357-67. [CrossRef]
3. Parkinson D. A surgical approach to the cavernous portion of the carotid artery: anatomical studies and case report. J Neurosurg 1965;23(5):474-83. [CrossRef]
4. Parkinson D. Transcavernous repair of carotid cavernous fistula. J Neurosurg 1967;26(4):420-4. [CrossRef]
5. Rhoton ALjr: The middle cranial base and cavernous sinus. In Dolenc VV, Rogers L (eds), Cavernous Sinus: Developments and Future Perspectives. Wien, Springer Verlag, 2009;3-25. [CrossRef]
6. Romero FR, Ramires D, Cristiano LC, Silva MP, Vieira RB. Endoscopic and microsurgical approaches to the cavernous sinus - Anatomical review. Arq Bras Neurocir 2017;36(3):160-6. [CrossRef]
7. Harris FS, Rhoton ALjr. Anatomy of the cavernous sinus: a microsurgical study. J Neurosurg 1976;45(2):169-80. [CrossRef]
8. Inoue T, Rhoton ALjr, Theele D, Barry ME. Surgical approaches to the cavernous sinus: a microsugical study. Neurosurgery 1990;26(6):903-932. [CrossRef]

9. Kayalioglu G, Govsa F, Erturk M, Pinar Y, Ozer MA, Ozgur T. The cavernous sinus: topographic morphometry of its contents. Surg Radiol Anat 1999;21(4):255-60. [CrossRef]
10. Lang J, Reiter U. Über den verlauf der hirnnerven in der seitenwand des sinus cavernosus. Neurochirurgia 1984;27(4):93-7. [CrossRef]
11. Miyazaki Y, Yamamoto I, Shinozuka T, Sato O. Microsurgical anatomy of the cavernous sinus. Neurol Med Chir 1994;34(3):150-63. [CrossRef]
12. Sekhar LN, Burges J, Akın O. Anatomical study of the cavernous sinus emphasizing operative approaches and related vascular and neural reconstruction. Neurosurgery 1987;21(6):806-16. [CrossRef]
13. Watanabe A, Nagaseki Y, Ohkubo S, Ohhashi Y, Horikoshi T, Nishigaya K et al. Anatomical variations of the ten triangles around the cavernous sinus. Clin Anat 2003;16(1):9-14. [CrossRef]
14. Keller JT, Leach JL, van Loveren HR, Abdel Aziz KM, Froelich S: Venous anatomy of the lateral sellar compartment. In Dolenc VV, Rogers L (eds), Cavernous Sinus: Developments and Future Perspectives. Wien, Springer Verlag, 2009;35-51. [CrossRef]
15. Suzuki Y, Matsumoto K. Variations of the superficial middle cerebral vein: Classification using three-dimensional CT angiography. Am J Neuroradiol 2000;21(5):932-8.
16. Gürses İA, Coşkun O, Öztürk A. Current status of cadaver sources in Turkey and a wake-up call for Turkish Anatomists. Anat Sci Educ 2018;11(2):155-65. [CrossRef]
17. Sanan A, Abdel Aziz KM, Janjua RM, van Loveren HR, Keller JT. Colored silicone injection for use in neurosurgical dissections: Anatomic technical note. Neurosurgery 1999;45(5):1267-71. [CrossRef]
18. Rasband WS. ImageJ, U.S. National Institutes of Health, Bethesda, Maryland, USA, 1997-2016 https://imagej.nih.gov/ij/ [accessed 21 September 2019]
19. Dalgıç A, Boyacı S, Aksoy K. Anatomical study of the cavernous sinus emphasizing operative approaches. Turk Neurosurg 2010;20(2):186-204. [CrossRef]
20. Chotai S, Liu Y, Qi S. Review of surgical anatomy of the tumors involving cavernous sinus. Asian J Neurosurg 2018;13(1):1-8. [CrossRef]
21. Heth JA, Al-Mefty O. Cavernous sinus meningiomas. Neurosurg Focus 2003;14(6):e3. [CrossRef]
22. Komatsu F, Komatsu M, Inoue T, Tschabitscher M. Endoscopic supraorbital extradural approach to the cavernous sinus: A cadaver study. J Neurosurg 2011;114(5):1331-7. [CrossRef]
23. Knosp E, Perneczky A, Koos WT, Fries G, Matula C. Meningiomas of the space of the cavernous sinus. Neurosurg 1996;38(3):434-44. [CrossRef]
24. Sun DQ, Menezes AH, Howard MA, Gantz BJ, Hasan DM, Hansen MR. Surgical management of tumors involving Meckel's cave and cavernous sinus: Role of an extended middle fossa and lateral sphenoidectomy approach. Otol Neurotol 2018;39(1):82-91. [CrossRef]
25. Dolci RLL, Upadhyay S, Filho LFSD, Fiore ME, Buohliqah L, Lazarini PR et al. Endoscopic endonasal study of the cavernous sinüs and quadrangular space: Anatomic relationships. Head Neck 2016;38(Suppl-1):E1680-7. [CrossRef]
26. Koutourousiou M, Filho FVG, Fernandez-Miranda JC, Wang EW, Stefko ST, Snyderman CH et al. Endoscopic endonasal surgery for tumors of the cavernous sinus: A series of 234 patients. World Neurosurg 2017;103:713-32. [CrossRef]
27. Theodosopoulos PV, Cebula H, Kurbanov A, Cabero AB, Osorio JA, Zimmer LA et al. The medial extra-sellar corridor to the cavernous sinus: Anatomic description and clinical correlation. World Neurosurg 2016;96:417-22. [CrossRef]
28. Woodworth GF, Patel KS, Shin B, Burkhardt JK, Tsiouris AJ, McCoul ED et al. Surgical outcomes using a medial-to-lateral endonasal endoscopic approach to pituitary adenomas invading the cavernous sinus. J Neurosurg 2014;120(5):1086-94. [CrossRef]
29. Day JD, Tschabitscher M: Microsurgical dissection of the cranial base. Churchill Livingstone, New York, 1996.
30. Samii M, Gerganov VM: Surgery of cavernous sinus meningiomas: Advantages and disadvantages. In Dolenc VV, Rogers L (eds), Cavernous Sinus: Developments and Future Perspectives. Wien, Springer Verlag, 2009;153-62. [CrossRef]
31. Tanoue S, Kiyosue H, Okahara M, Sagara Y, Hori Y, Kashiwagi J et al. Para-cavernous sinus venous structures: Anatomic variations and pathologic conditions evaluated on fat-suppressed 3D fast gradient-echo MR images. Am J Neuroradiol 2006;27(5):1083-89.
32. Chung BS, Ahn YH, Park JS. Ten triangles around cavernous sinus for surgical approach, described by schematic diagram and three dimensional models with the sectioned images. J Korean Med Sci 2016;31(9):1455-63. [CrossRef]
33. Park JS, Chung MS, Shin DS, Har DH, Cho ZH, Kim YB et al. Sectioned images of the cadaver head including the brain and correspondences with ultrahigh field 7 T MRIs. Proc IEEE 2009;97(12):1988-96. [CrossRef]
34. Park HS, Chung MS, Shin DS, Jung YW, Park JS. Whole courses of the oculomotor, trochlear, and abducens nerves, identified in sectioned images and surface models. Anat Rec 2015;298(2):436-43. [CrossRef]
35. Hakuba A, Tanaka K, Suzuki T, Nishimura S. A combined orbitozygomatic infratemporal epidural and subdural approach for lesions involving the entire cavernous sinus. J Neurosurg 1989;71(5Pt1):699-704. [CrossRef]
36. Qian ZH, Feng X, Li Y, Tand K. Virtual reality model of the three-dimentional anatomy of the cavernous sinus based on a cadaveric image and dissection. J Craniofac Surg 2018;29(1):163-6. [CrossRef]